JOURNAL OF NEUROTRAUMA 33:1645–1649 (September 1, 2016)

DOI: 10.1089/neu.2015.4107

Short Communication

Mild Traumatic Brain Injury Decreases Broadband Power in Area CA1

Rosalia Paterno,[1] Hannah Metheny,[2] Guoxiang Xiong,[2] Jaclynn Elkind,[2] and Akiva S. Cohen[2,3]

Abstract

Cognitive impairment caused by traumatic brain injury (TBI) can lead to devastating consequences for both patients and their families. The underlying neurological basis for TBI-induced cognitive dysfunction remains unknown. However, many lines of research have implicated the hippocampus in the pathophysiology of TBI. In particular, past research has found that theta oscillations, long thought to be the electrophysiological basis of learning and memory, are decreased in the hippocampus post-TBI. Here, we recorded *in vivo* electrophysiological activity in the hippocampi of 16 mice, 8 of which had previously undergone a TBI. Consistent with previous data, we found that theta power in the hippocampus was decreased in TBI animals compared to sham controls; however, this effect was driven by changes in broadband power and not theta oscillations. This result suggests that broadband fluctuations in the hippocampal local field potential can be used as an electrophysiological surrogate of abnormal neurological activity post-TBI.

Key words: hippocampus; *in vivo* recording; theta rhythm; traumatic brain injury

Introduction

Traumatic brain injury (TBI) leads to a unique set of symptoms that afflict patients after exposure to head trauma. Lateral fluid percussion injury (LFPI) is a widely accepted, reproducible experimental rodent model of TBI.[1–3] Previous research has shown that TBI leads to hippocampal damage[4,5] that is associated with a disruption of the balance between excitatory and inhibitory (E-I) neural activity.[6–8] To link these changes to the clinical syndrome of TBI, it is necessary to obtain an *in vivo* proxy of E-I (im)balance. To that end, neural oscillations of the local field potential can be used as a metric of excitatory and inhibitory neural transmission over a specific region of neural tissue, such as the hippocampus, in the awake behaving animal.[9] Indeed, previous research has shown that a decrease in hippocampal theta oscillations is a marker of TBI.[10,11] However, it remains unclear whether faster oscillations, which are also generated by the balance between excitatory and inhibitory neural activity,[9,12–17] are altered post-TBI.

Methods

To investigate the relation between oscillations at all frequency bands and TBI, 16 (5–8 weeks old, 24–28 g) C57BL/6J male mice (The Jackson Laboratory, Bar Harbor, ME) were anesthetized (ketamine and xylazine mixture) and LFPI was performed, as previously described.[6] All experimental procedures and protocols for animal studies were approved by the Children's Hospital of Philadelphia's Institutional Animal Care and Use Committee in accord with the international guidelines on the ethical use of animals (National Research Council, National Academy Press, Washington DC, 1996).[8] On day 1, a craniectomy was performed over the right parietal area between bregma and lambda keeping the dura intact. On day 2, the injury was induced by a brief pulse of saline onto the intact dura at a pressure of 1.5 atm, generating a mild brain injury. Sham animals received all of the above procedures except the fluid pulse.

Six to 8 days post-LFPI, injured ($n = 8$) and respective time-matched sham ($n = 8$) animals were reanesthetized (ketamine and xylazine), and three electrodes (monopolar 0.004 inch stainless steel; A-M Systems, Carlsborg, WA) were guided into the hippocampal area CA1 using stereotaxic coordinates (2.2 mm posterior to the bregma, 2 mm lateral to the midline; see Fig. 1A). The recording electrodes were implanted only ipsilateral to the injury location directly above the craniectomy. A reference and ground electrode were placed in the cerebellum and in the skull behind the lambda suture, respectively. Two support screws were positioned over the anterior aspect of the skull, and the entire ensemble was secured with dental cement (Plastick One, Roanoke, VA).

Post-surgery, all animals were allowed to recover on an electric heating pad until spontaneously mobile and were returned to their home cage. After at least 24 h, animals were transferred to the recording cage (same dimensions as the home cage). Animals were allowed free access to food and water in the recording cage. *In vivo* recordings were obtained for at least 24 h. All encephalography (EEG) recordings were performed at 8–10 days post-LFPI. All

[1]Center for Sleep and Circadian Neurobiology, Hospital of the University of Pennsylvania, Philadelphia, Pennsylvania.
[2]Joseph Stoke's Research Institute, Children's Hospital of Philadelphia, Department of Anesthesiology, Philadelphia, Pennsylvania.
[3]Department of Anesthesiology, Perelman School of Medicine, University of Pennsylvania, Philadelphia, Pennsylvania.

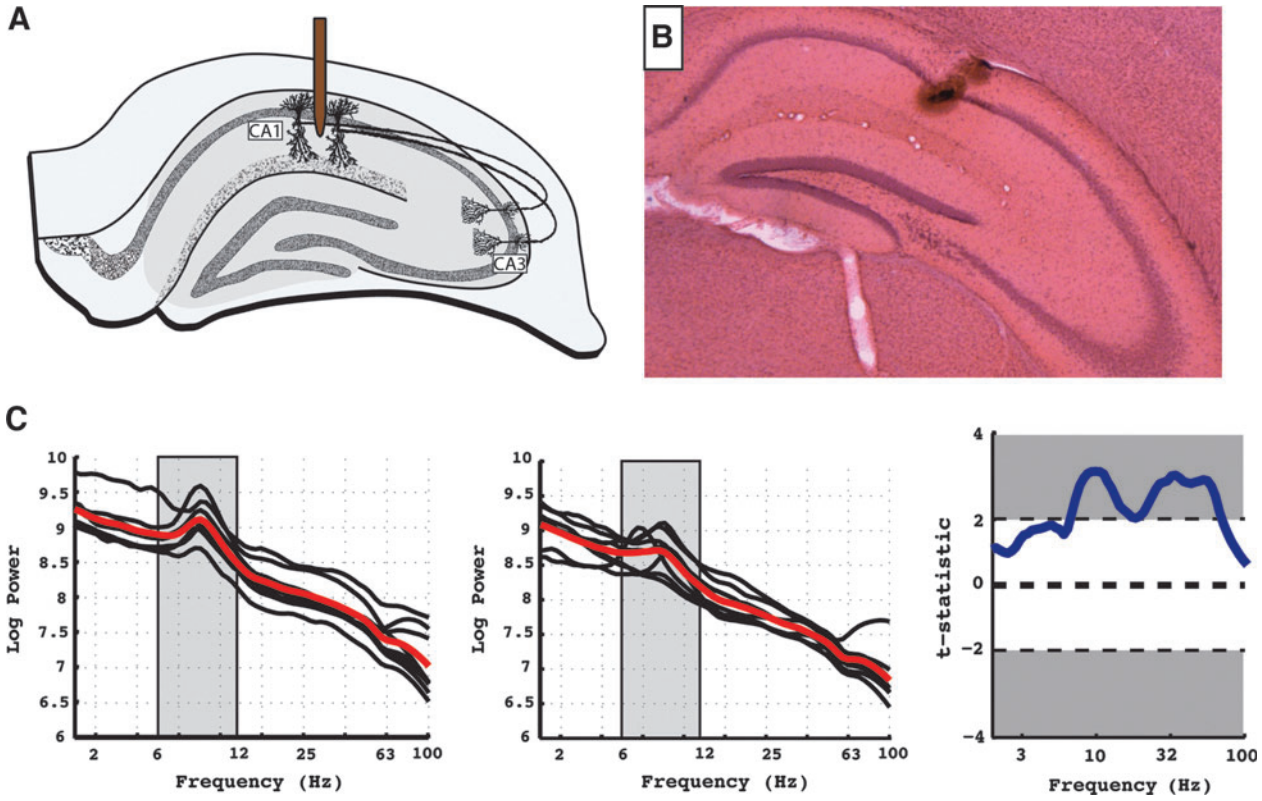

FIG. 1. Electrode implantation, locations, and power spectra. (**A**) The target location of the microelectrode in area CA1 is shown on a schematic of the rodent hippocampus. (**B**) An example of the actual location of the target electrode on a histological stain of rodent hippocampus. (**C**) Left panel: the power spectra for all mice in the sham condition. Black lines represent the averaged power spectra across all time epochs for each animal. The red line represents the average power spectra across all animals in each condition. The gray box represents the theta frequency range (6–12 Hz). All power spectra were log transformed before averaging across epochs. Middle panel: identical plot for TBI animals. Right panel: Power differences for all frequencies were assessed with a two-way *t*-test, and the *t*-statistic is shown for each frequency on the y-axis. A positive *t*-statistic suggests that there is more power in the sham animals than the TBI animals at the given frequency. Error bars represent standard error of the mean. Significant regions ($p < 0.05$) are shown in gray. TBI, traumatic brain injury. Color image is available online at www.liebertpub.com/neu

recordings were performed using a Stellate-Harmonie (Stellate Inc., Montreal, Quebec Canada) 16-bit, 24-channel digital EEG amplifier, sampling at 2000 Hz with a hardware 1000-Hz low-pass antialiasing filter. Unity gain pre-amplifiers were constructed in-house from TI LM2478 quad operational amplifier integrated circuits (Texas Instruments, Dallas, TX). After recording, animals were sacrificed and processed for histological assessment of electrode location. Animals were anesthetized with 5% chloral hydrate, and the electrode positions were marked by passing 15 μA for 15 sec through each electrode (Fig. 1B). Immediately after current injection, animals were perfused with saline followed by 3% paraformaldehyde (PFA; Sigma-Aldrich, St. Louis, MO). Brains were post-fixed with PFA 3%, and 50-μm-thick coronal sections were cut with a VT 1000S vibratome (Leica Microsystems Inc., Buffalo Grove, IL).

The recorded local field potential was analyzed post hoc in the following manner. First, video of the rodents was manually parsed and periods of exploration, defined as sniffing and/or walking, were selected. From these exploratory time periods, the data were further segmented into nonoverlapping epochs of 3000 msec duration. These epochs consisted of 2000 msec duration with two 500-msec flanking buffers on each end in order to diminish edge effects during the analysis. To generate an instantaneous power and phase spectrum, these epochs of EEG were convolved with a bank of 100 Morlet wavelet filters, logarithmically spaced from 2 to 800 Hz.[18] For the power analyses, we averaged the instantaneous, log-transformed, power across the 2000 msec interval to obtain an estimate of the power spectrum for that trace. The power spectrum for each animal was determined by averaging each power spectrum across all time epochs for each animal. We compared the distribution of average power spectra across TBI and sham conditions using a two-tailed *t*-test.

Results

Our goal was to investigate whether power fluctuations were attributable to specific narrow-band neural oscillations or broadband shifts in power. To separate broadband changes in power from narrow band, we employed the method described by Manning and colleagues. Specifically, we performed a robust regression of the log-power values as a function of log-transformed frequency across all time epochs and then subtracted the power values from this regression line to remove the effect of broadband shifts in power on the spectrum.[19]

Using this approach, we first attempted to recapitulate the previous result that theta power in the rodent hippocampus is reduced post-LFPI.[10,11] In Figure 1C, the power spectrum averaged across recording epochs is shown for each animal in both the sham (Fig. 1C, left-most panel) and TBI condition (Fig. 1C, middle panel). There is a clear peak in the power spectra in the theta range

(6–12 Hz), which appears to have a higher absolute amount of power in the sham condition compared to TBI. To test this, we separately averaged the power in the theta range for each animal and directly compared the amount of theta power in the TBI and sham conditions. We found that theta power is significantly decreased in TBI relative to the sham control ($p < 0.05$; *t*-test), consistent with previous work.[10,11]

We next repeated the comparison of power values in the TBI and sham condition for all frequency bands. Figure 1C (right-most panel) shows the *t*-statistics comparing power for all frequencies from this comparison. In the figure, a larger *t*-statistic (y-axis) suggests there was more power in the sham versus TBI population at the associated frequency (x-axis). The analysis further confirms that all frequencies, not just theta, demonstrated a decrease in power post-TBI. We hypothesized that TBI causes both a decrease in theta oscillations and a decrease in broadband power. The former has been linked to E-I balance,[9] and the latter likely reflects large-scale changes in multi-unit activity.[19,20]

To resolve this issue, we implemented the method of Manning and colleagues, which uses a robust regression on the log-log plot of the power spectrum to subtract broadband power from narrow band power (i.e., neural oscillations of specific frequencies). This method is illustrated for the power spectrum of a representative single animal in the sham population (see Fig. 2A). Figure 2A (left-most plot) shows the original power spectrum, which represents an average of the power spectra from all time epochs during which the animal was exploring. Figure 2A (middle panel) shows the actual power values for all such time epochs as black dots: each frequency (x-axis) has a distribution of black dots along the y-axis that represents the power values for all time epochs. A robust regression was then run with frequency as the independent variable and power as the dependent variable (red line). Then, each individual power value (black dots) was subtracted from the regression output (red line) to obtain the residual values at each time epoch. These residuals were then averaged across all time epochs to yield the broadband corrected power (Fig. 2A, right-most panel). This method separates the contribution of broadband power and oscillatory power to the overall power spectrum.[19]

We then applied this technique to the data from all animals in the sham (Fig. 2B, left-most panel) and TBI (Fig. 2B, middle-panel) groups. The figure demonstrates that, after the correction for broadband power changes, 1) the baselines of the power spectrum are normalized and 2) the change in theta power across the groups is greatly diminished. To quantify this, we averaged the amount of residual power in the theta band in both TBI and sham conditions; this analysis showed that there is no significant difference in the amount of theta in the two conditions, although the theta in the TBI condition was lower than the sham condition ($p < 0.15$; *t*-test; Fig. 2B, right-most plot; gray bars). However, when we directly compared the amount of broadband power between the two conditions, there was a significant ($p < 0.05$; *t*-test) decrease in

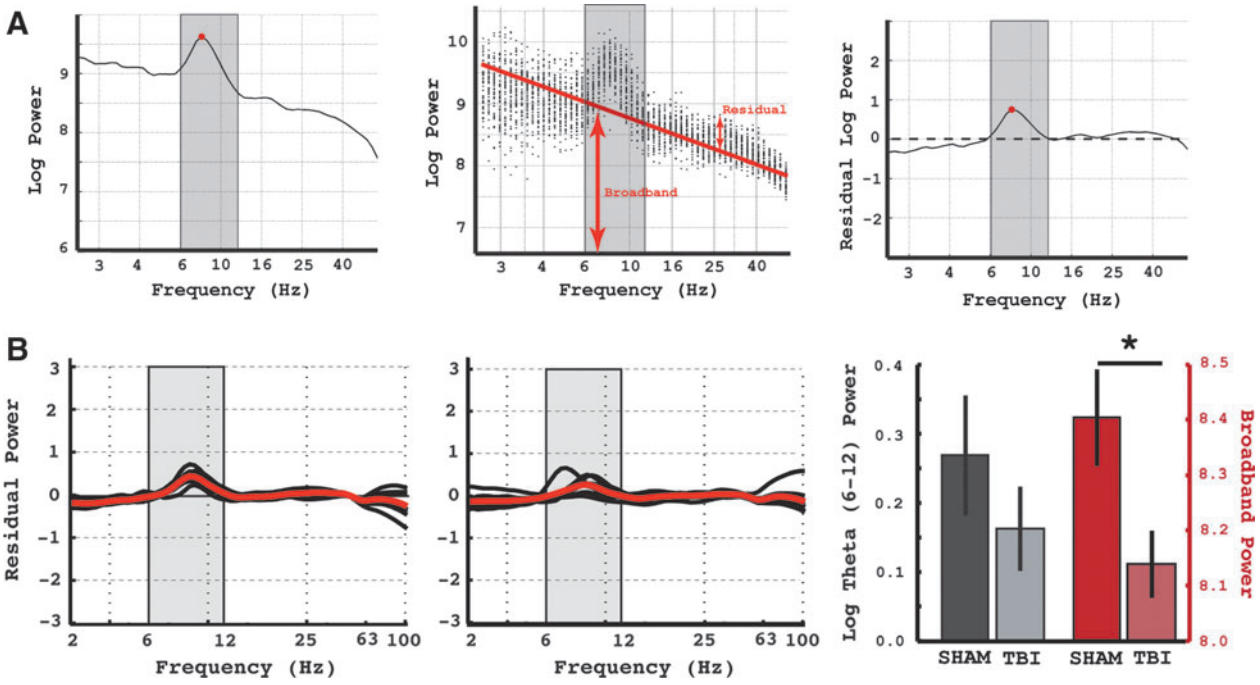

FIG. 2. Broadband correction. (**A**) Left panel: The averaged power spectrum of 1 animal in the sham condition is shown. The red dot represents the peak frequency of the theta oscillation for that animal, which, in this case, was 8.17 Hz. Middle panel: The distribution of power values across all time epochs are shown. The red line represents a regression through the distribution of power values. The broadband power is represented by the height of the red line. The residuals (regression line subtracted from the power values) represent the broadband correction. Right panel: The average broadband correction across all time epochs. The theta oscillation remains and can be seen as a bump in the spectrum that has been separated from the broadband component of the original spectrum. (B) Left-panel: The broadband corrected power spectra for sham animals. The red line represents the average across all animals. The gray box represents the theta frequency range (6–12 Hz). Middle panel: identical plot for TBI animals. Right panel: Averaged broadband corrected residual theta power (left side, gray box) and averaged total broadband power (right side, red boxes) was computed separately and compared for sham and TBI animals. Error bars represent standard error of the mean. Asterisk represents a significant difference between sham and TBI conditions (two-sample *t*-test); $p < 0.05$. TBI, traumatic brain injury. Color image is available online at www.liebertpub.com/neu

broadband power in the TBI condition compared to the sham condition (Fig. 2B, right-most plot; red bars).

Discussion

Broadband power has been shown to reflect the overall multi-unit activity (MUA) in the region surrounding the microelectrode[19,20]; thus, the most basic interpretation of these data is that the decrease in broadband power post-TBI reflects a decrease in MUA in area CA1 post-LFPI. Interestingly, this basic interpretation is not consistent with previous work showing that the overall firing rate in the rodent hippocampus is unchanged post-TBI. [21] However, bursting activity in CA1 is reliably reduced post-TBI.[22] It has previously been shown that MUA correlates with broadband activity more closely during periods when the neurons in the local population are highly correlated.[23] We suggest that a change in the overall level of neuronal correlation post-TBI may explain the decrease in bursts and broadband activity.

Although many studies have provided evidence for[19,20] and suggested that[26,27] broadband activity correlates strongly with the underlying firing rate, this point remains controversial. Specifically, Ekstrom and colleagues[28] found that spike rate in the hippocampus was not directly related to any frequency activity in the local field potential. This controversy may be explained by the finding that the correlation between spike rate and broadband changes is dependent on the level of interneuronal correlations between neurons.[23] This fits with our proposal that, during injury, neurons become less correlated (i.e., more asynchronous), thereby decreasing the overall level of broadband power. In order to test this hypothesis, it is necessary to record from multiple neurons simultaneously post-TBI, which has not previously been attempted *in vivo*.

An alternate hypothesis is that LFPI causes neuronal loss in the ipsilateral hippocampus. This neuronal loss could lead to diminish overall firing and thus a decrease in broadband power. Indeed, previous work using more moderate injury severities, have demonstrated a loss of CA3 neurons at the site of injury, consistent with this hypothesis.[24] However, it is important to note that our LFPI is induced with injury pressures at 1.5 atm. At this level of injury, no visible loss of neurons in the hippocampus has been demonstrated.[21,25] Further, previous *in vivo* hippocampal recording has shown no change in overall firing rate after mild TBI as compared to sham controls.[21] Thus, our decrease in broadband activity is likely the result of another pathological process independent from simple neuronal loss.

Lee and colleagues[29] have also used a broadband correction to show that theta oscillations correlate with the injured state. By correcting for broadband power, this study elegantly demonstrates that theta oscillations are affected by injury. Our article adds to this result in two ways. First, by using the Manning-Kahana regression method to correct for broadband power, we were able to show that broadband power itself correlates more strongly with the injured state than theta oscillations. Second, we conducted our experiments using a mild TBI (1.5 atm injury) as compared to the moderate injury (2.2 atm) used in Lee and colleagues.[29] It may be that these two injury severities have different electrophysiological correlates, which would indicate that mild TBI is a unique disease and not a mild version of more severe TBI. Future research should compare how the severity of injury affects *in vivo* electrophysiological activity.

Finally, we note that the dimensions of the cage were chosen to allow the animals to quickly habituate to the environment. This resulted in maximal exploration and sniffing behaviors. However, a significant consequence of the small size was that mice were unable to accelerate to running speeds, which are associated with unique theta signatures.[30] Therefore, it is possible that the lack of a correlation between theta oscillatory activity and exploration stems from the fact that the animals could not run during our paradigm. Further research is needed to determine the specific animal behaviors and features of theta that are damaged post-TBI.

Acknowledgments

This work was supported by the National Institute of Child Health and Human Development at the National Institutes of Health (R37-HD059288; to A.S.C.) and the National Institute of Neurological Disease and Stroke at the National Institutes of Health (R01-NS069629; to A.S.C.). The authors thank Eric Marsh for helpful discussion and input.

Author Disclosure Statement

No competing financial interests exist.

References

1. Dixon, C.E., Lyeth, B.G., Povlishock, J.T., Findling, R.L., Hamm, R.J., Marmarou, A., and Hayes, R.L. (1987). A fluid percussion model of experimental brain injury in the rat. J. Neurosurg. 67, 110–119.
2. McIntosh, T.K., Noble, L., Andrews, B., and Faden, A.I. (1987). Traumatic brain injury in the rat: characterization of a midline fluid-percussion model. Cent. Nerv. Syst. Trauma 4, 119–134.
3. Smith, D.H., Okiyama, K., Thomas, M.J., Claussen, B., and McIntosh, T.K. (1991). Evaluation of memory dysfunction following experimental brain injury using the Morris water maze. J. Neurotrauma 8, 259–269.
4. Reeves, T.M., Lyeth, B.G., Phillips, L.L., Hamm, R.J., and Povlishock, J.T. (1997). The effects of traumatic brain injury on inhibition in the hippocampus and dentate gyrus. Brain Res. 757, 119–132.
5. Santhakumar, V., Ratzliff, A.D., Jeng, J., Toth, Z., and Soltesz, I. (2001). Long-term hyperexcitability in the hippocampus after experimental head trauma. Ann. Neurol. 50, 708–717.
6. Witgen, B.M., Lifshitz, J., Smith, M.L., Schwarzbach, E., Liang, S.L., Grady, M.S., and Cohen, A.S. (2005). Regional hippocampal alteration associated with cognitive deficit following experimental brain injury: a systems, network and cellular evaluation. Neuroscience 133, 1–15.
7. Cole, J.T., Mitala, C.M., Kundu, S., Verma, A., Elkind, J.A., Nissim, I., and Cohen, A.S. (2009). Dietary branched chain amino acids ameliorate injury-induced cognitive impairment. Proc. Natl. Acad. Sci. 107, 366–371.
8. Johnson, B.N., Palmer, C.P., Bourgeois, E.B., Elkind, J.A., Putnam, B.J., and Cohen, A.S. (2014). Augmented inhibition from cannabinoid-sensitive interneurons diminishes CA1 output after traumatic brain injury. Front. Cell. Neurosci. 8, 1–19.
9. Atallah, B.V., and Scanziani, M. (2009). Instantaneous modulation of gamma oscillation frequency by balancing excitation with inhibition. Neuron 62, 566–577.
10. Fedor, M., Berman, R.F., Muizelaar, J.P., and Lyeth, B.G. (2010). Hippocampal theta dysfunction after lateral fluid percussion injury. J. Neurotrauma 27, 1605–1615.
11. Lee, D.J., Gurkoff, G.G., Izadi, A., Berman, R.F., Ekstrom, A.D., Muizelaar, J.P., and Shahlaie, K. (2013). Medial septal nucleus theta frequency deep brain stimulation improves spatial working memory after traumatic brain injury. J. Neurotrauma 30, 131–139.
12. Gray, C.M. (1994). Synchronous oscillations in neuronal systems: mechanisms and functions. J. Comput. Neurosci. 1, 11–38.
13. Bragin, A., Jandó, G., Nádasdy, Z., Hetke, J., Wise, K., and Buzsáki, G. (1995). Gamma (40–100 Hz) oscillation in the hippocampus of the behaving rat. J. Neurosci. 15, 47–60.
14. Traub, R.D., Whittington, M.A., Colling, S.B., Buzsáki, G., and Jefferys, J.G. (1996). Analysis of gamma rhythms in the rat hippocampus in vitro and in vivo. J. Physiol. 493, 471–484.

15. Whittington, M.A., Traub, R.D., Kopell, N., Ermentrout, B., and Buhl, E.H. (2000). Inhibition-based rhythms: experimental and mathematical observations on network dynamics. Int. J. Psychophysiol. 38, 315–336.
16. Bartos, M., Vida, I., and Jonas, P. (2007). Synaptic mechanisms of synchronized gamma oscillations in inhibitory interneuron networks. Nat. Rev. Neurosci. 8, 45–56.
17. Tiesinga, P., and Sejnowski, T.J. (2009). Cortical enlightenment: are attentional gamma oscillations driven by ING or PING? Neuron 63, 727–732.
18. Addison, P.S. (2002). *The Illustrated Wavelet Transform Handbook: Introductory Theory and Applications in Science, Engineering, Medicine and Finance*. CRC Press: Boca Raton, FL.
19. Manning, J.R., Jacobs, J., Fried, I., and Kahana, M.J. (2009). Broadband shifts in local field potential power spectra are correlated with single-neuron spiking in humans. J. Neurosci. 29, 13613–13620.
20. Ray, S., and Maunsell, J.H. (2011). Different origins of gamma rhythm and high-gamma activity in macaque visual cortex. PLoS Biol. 9, e1000610.
21. Eakin, K., and Miller, J.P. (2012). Mild traumatic brain injury is associated with impaired hippocampal spatiotemporal representation in the absence of histological changes. J. Neurotrauma 29, 1180–1187.
22. Munyon, C., Eakin, K.C., Sweet, J.A., and Miller, J.P. (2014). Decreased bursting and novel object-specific cell firing in the hippocampus after mild traumatic brain injury. Brain Res. 1582, 220–226.
23. Nir, Y., Fisch, L., Mukamel, R., Gelbard-Sagiv, H., Arieli, A., Fried, I., and Malach, R. (2007). Coupling between neuronal firing rate, gamma LFP, and BOLD fMRI is related to interneuronal correlations. Curr. Biol. 17, 1275–1285.
24. Smith, D.H., Okiyama, K., Thomas, M.J., Claussen, B., and McIntosh, T.K. (1991). Evaluation of memory dysfunction following experimental brain injury using the Morris water maze. J. Neurotrauma 8, 259–269.
25. Hylin, M.J., Orsi, S.A., Zhao, J., Bockhorst, K., Perez, A., Moore, A.N., and Dash, P.K. (2013). Behavioral and histopathological alterations resulting from mild fluid percussion injury. J. Neurotrauma 30, 702–715.
26. Miller, K.J., Leuthardt, E.C., Schalk, G., Rao, R.P., Anderson, N.R., Moran, D.W., and Ojemann, J.G. (2007). Spectral changes in cortical surface potentials during motor movement. J. Neurosci. 27, 2424–2432.
27. Ray, S., and Maunsell, J.H. (2015). Do gamma oscillations play a role in cerebral cortex? Trends Cogn. Sci. 19, 78–85.
28. Ekstrom, A., Viskontas, I., Kahana, M., Jacobs, J., Upchurch, K., Bookheimer, S., and Fried, I. (2007). Contrasting roles of neural firing rate and local field potentials in human memory. Hippocampus 17, 606.
29. Lee, D.J., Gurkoff, G.G., Izadi, A., Seidl, S.E., Echeverri, A., Melnik, M., Berman, R.F., Ekstrom, A.D., Muizelaar, J.P., Lyeth, B.G., and Shahlaie, K. (2015). Septohippocampal neuromodulation improves cognition after traumatic brain injury. J. Neurotrauma 32, 1822–1832.
30. Hinman, J.R., Penley, S.C., Long, L.L., Escabí, M.A., and Chrobak, J.J. (2011). Septotemporal variation in dynamics of theta: speed and habituation. J. Neurophysiol. 105, 2675–2686.

Address correspondence to:
Akiva S. Cohen, PhD
Department of Anesthesiology and Critical Care Medicine
Perelman School of Medicine
University of Pennsylvania
Children's Hospital of Philadelphia
Abramson Research Center
Room 816-h
3615 Civic Center Boulevard
Philadelphia, PA 19104-4399

E-mail: cohena@email.chop.edu